

УДК 539.12: 539.171

## SINGLE-SPIN ASYMMETRIES AT CLAS

*H. Avakian, L. Elouadrhiri\**

*for the CLAS Collaboration, Jefferson Laboratory, USA*

We present recent results from Jefferson Lab's CLAS detector on beam and target single-spin asymmetries in single-pion electroproduction off unpolarized hydrogen and polarized  $\text{NH}_3$  targets. Systematic studies of factorization of  $x$  and  $z$  dependences have been performed for different spin-dependent and independent observables. No significant  $x/z$  dependence has been observed within statistical uncertainties, which is consistent with factorization holding within the kinematic range and the precision of the present measurement. Nonzero single-beam and single-target spin asymmetries have been observed for the first time in semi-inclusive and exclusive pion production in hard-scattering kinematics.

Представлены последние экспериментальные данные CLAS по одиночным асимметриям одиночных пионов на поляризованных пучках и неполяризованной водородной и поляризованной  $\text{NH}_3$ -мишенях. Систематически исследовалась факторизация  $x$  и  $z$ , никакого значимого ее нарушения не обнаружено. Впервые наблюдались ненулевые асимметрии полунклюзивных и эксклюзивных пионов в кинематике жесткого рассеяния.

The orbital momentum of partons has been of central interest ever since the EMC [1] measurements implied that the constituent quarks account for only a fraction of the nucleon spin. Transverse momentum of quarks is a key to orbital angular momentum. In recent years parton distribution functions have been generalized to contain information not only on the longitudinal but also on the transverse distributions of partons in a fast moving hadron. New distribution functions, namely Generalized Parton Distributions (GPDs) [2–4] and Transverse Momentum-Dependent distribution functions (TMDs) [5–15] added important pieces of information missing in one-dimensional parton densities, in particular distribution of partons in the plane transverse to the direction of motion and their transverse momentum distributions. Finally the phase-space Wigner distributions were introduced [16] containing most general one-body information of protons. After integration over the spatial coordinates, they reduce to TMDs and after integration over the transverse momentum and a specific Fourier transform they recover the GPDs. In recent years it has become clear that appropriate exclusive and semi-inclusive scattering processes may provide access to these two sets of generalized parton distributions.

---

\*Talk presented by Peter Bosted.

Eight independent TMDs were identified [5, 8, 10] at leading twist, with the transverse momentum  $k_T$  of partons included, which are accessible in semi-inclusive deep inelastic scattering. They make possible studies of transitions of nucleons with one polarization state to a quark with another polarization state. In particular, the  $f_{1T}^\perp$  and  $h_1^\perp$  known as the Sivers and Boer functions [6, 10–15] describe unpolarized quarks in the transversely polarized nucleon and transversely polarized quarks in the unpolarized nucleon respectively. They are *time-reversal odd* ( $T$ -odd) and require final state interactions and interference between different helicity states. Another important quantity accessible in SSA measurements is the Mulders leading-twist distribution function  $h_{1L}^\perp$  [8] describing transversely polarized quarks in the longitudinally polarized nucleon. Similar quantities arise in the hadronization process. One particular case is the Collins  $T$ -odd fragmentation function  $H_1^\perp$  [7] describing fragmentation of transversely polarized quarks into unpolarized hadrons. As shown recently in Ref. 15, the interaction between the active parton in the hadron and the target spectators [12, 14, 17] leads to gauge-invariant transverse momentum-dependent (TMD) parton distributions.

Single-spin asymmetries (SSA) in hadronic reactions have been among the most difficult phenomena to understand from first principles in QCD. Large SSAs have been observed in hadronic reactions for decades [18, 19]. Recently, significant SSAs were reported in semi-inclusive DIS (SIDIS) by the HERMES Collaboration at HERA [20, 21] for a longitudinally polarized target, by the SMC Collaboration at CERN for a transversely polarized target [22], and by the CLAS Collaboration at the Thomas Jefferson National Accelerator Facility (JLab) with a polarized beam [23]. In general, such single-spin asymmetries require a correlation of a particle spin direction and the orientation of the production or scattering plane. In hadronic processes, such correlations can provide a window into the physics of initial and final state interactions at the parton level.

This contribution presents measurements of single-spin asymmetries in exclusive and semi-inclusive processes in hard-scattering kinematics using a 5.7 GeV electron beam and the CEBAF Large Acceptance Spectrometer (CLAS) [27] at JLab. Scattering of longitudinally polarized electrons off a 5-cm-long liquid-hydrogen target (e16 experiment) and off a polarized  $\text{NH}_3$  target (eg1 experiment) was studied over a wide range of kinematics. The average beam polarization, frequently measured with a Møller polarimeter, was  $0.73 \pm 0.03$  and the average target polarization for  $\text{NH}_3$  was  $0.72 \pm 0.05$ . The scattered electrons and pions were detected in CLAS [27]. The e16 data set corresponds to an integral luminosity of  $2.6 \cdot 10^{40} \text{ cm}^{-2}$ . The total number of events in the DIS range ( $Q^2 > 1.2 \text{ GeV}^2$ ,  $W^2 > 4 \text{ GeV}^2$ ) selected by quality, vertex, acceptance, fiducial, and kinematic cuts was  $\approx 7.8 \cdot 10^6$  for electron- $\pi^+$  coincidences and  $\approx 2.4 \cdot 10^6$  for electron-proton coincidences with no other charged particles in the detector.

## 1. FACTORIZATION STUDIES

Assuming that the quark scattering and fragmentation processes factorize, the cross section can be evaluated as the convolution of a distribution function depending on the Bjorken variable  $x$ , hard scattering part and the fragmentation function depending on the fraction of energy of the virtual photon  $z$  carried by the final-state hadron. In case of the unpolarized beam and target the cross section is given by [8]:

$$\sigma_{UU} \propto (2 - 2y + y^2) \sum_{q,\bar{q}} e_q^2 f_1^q(x) D_1^q(z), \quad (1)$$

where kinematic variables  $x$ ,  $y$ , and  $z$  are defined as:  $x = Q^2/2(P_1q)$ ,  $y = (P_1q)/(P_1k_1)$ , and  $z = (P_1P)/(P_1q)$ . The  $q = k_1 - k_2$  is the momentum of the virtual photon,  $Q^2 = -q^2$ ;  $P_1$  and  $P$  are the momenta of the target and the observed final-state hadron. The sum  $\sum_{q,\bar{q}}$  is over quark flavors,  $y$  and  $z$  are fractions of electron energy carried by the virtual photon and the fraction of the virtual photon energy carried by the pion, respectively. The  $f_1^q(x)$  and  $D_1^q(z)$  are the unpolarized distribution and fragmentation functions.

The  $x$  and  $z$  dependences of the total cross section are given by  $x$  dependence of the distribution function and  $z$  dependence of the fragmentation function. Studies of dependences on  $x$  and  $z$  of pions in SIDIS thus provide a simple test of factorization.

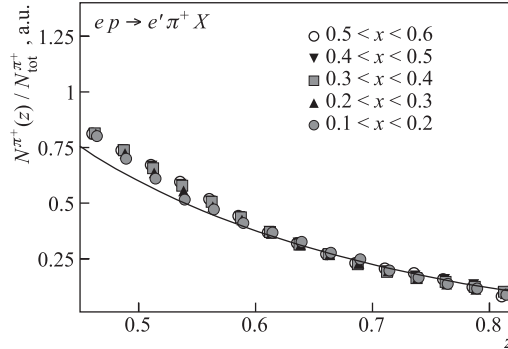


Fig. 1. Pion multiplicities as a function of  $z$  for different  $x$  ranges normalized by the total number of pions in the corresponding  $x$  range. The curve is the fragmentation function  $D_u^{\pi^+}$  from [26]

In Fig. 1 multiplicities normalized by total number of events are shown as a function of  $z$  for different  $x$  bins. Within the range and the precision of the present measurement no  $x$  dependence is appearing. This is consistent with factorization. The curve on Fig. 1 shows the fragmentation function by Kretzer et al. [26]. Radiative corrections and a small fraction of target fragmentation events may account for the major part of the difference at low  $z$ . The DIS interpretation is valid if the hadron originates from the fragmentation of the *current* quark. At low  $z$  hadrons may originate also from the fragmentation of the target, while at

large  $z$ , in addition to higher twist effects, diffractive events are also important. Therefore a restricted range in  $0.5 < z < 0.8$  has been selected for further analysis. The event distributions in the restricted  $z$  range have been compared with the Monte Carlo based on the LUND generator developed to describe high-energy processes. In LUND, the pion production in a chosen kinematic range is dominated by direct production from string fragmentation, as opposed to other processes like target fragmentation and hadronic decays.

Variety of possible observables to test the factorization is provided when measuring single and double polarized asymmetries as a function of  $x$  or  $z$  in different bins of  $z$  and  $x$ , respectively. Comparison of the CLAS data at 5.7 GeV with measurements performed at higher energies is also considered as an important step in ensuring that our studies in DIS kinematics are in fact related to the deep-inelastic scattering and could be analyzed in DIS terms.

In case of the polarized beam and target the cross section has contributions depending on the spin of the target or spin of the beam or both, involving various TMD distribution functions [8, 10, 24, 28]. The double polarized contribution is given by:

$$\sigma_{LL} \propto \lambda S_L y (2-y) \sum_{q,\bar{q}} e_q^2 g_1^q(x) D_1^q(z),$$

where  $\lambda$  and  $S_L$  are the beam and longitudinal target polarizations and  $g_1(x)$  is the helicity distribution, describing longitudinally polarized quarks in the longitudinally polarized proton.

The double polarized asymmetry  $A_1$  in particular is defined as  $\sigma_{LL}/\sigma_{UU}$  and its  $x$  dependence in case of  $u$ -quark dominance should not exhibit any  $z$  dependence if factorization is holding. The  $x$  dependence of  $A_1$  from CLAS

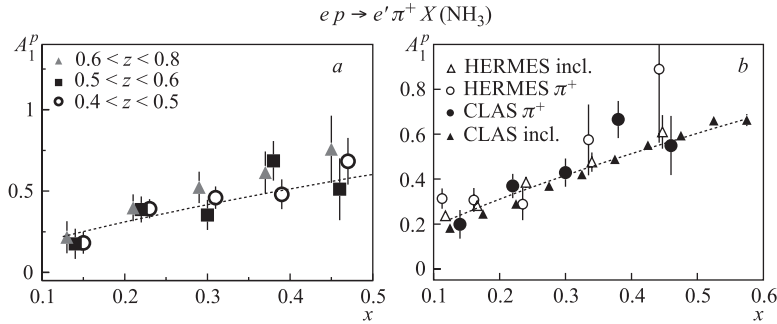


Fig. 2. The double-spin asymmetry as a function of  $x$  for different  $z$  ranges from CLAS 5.7 GeV polarized target data (a) and as a function of  $x$  for inclusive and semi-inclusive samples at CLAS and HERMES [35] (b)

polarized target data was extracted for different  $z$  bins and no significant variation was observed as a function of  $z$  within statistical uncertainties (see Fig. 2).

The comparison of CLAS double-spin asymmetry  $A_1$  with HERMES both for inclusive and semi-inclusive samples is shown in Fig. 2. The difference in evolutions of  $g_1(x, Q^2)$  and  $f_1(x, Q^2)$  distribution functions may account for most of the (15–20%) difference at low  $Q^2$  [36]. Otherwise double-spin asymmetries measured at different (factor of  $\sim 5$ ) beam energies and different  $Q^2$  (factor of  $\sim 3$ ) are in very good agreement indicating no significant  $Q^2$  or beam energy dependence of the double-spin asymmetry  $A_1$ .

## 2. SSA IN SIDIS WITH POLARIZED TARGET AND BEAM

For polarized targets, several azimuthal asymmetries already arise at leading order. The following contributions were investigated in Refs. 7–9, 17, 14, 33:

$$\sigma_{UL}^{\sin 2\phi} \propto S_L 2(1-y) \sin 2\phi \sum_{q,\bar{q}} e_q^2 x h_{1L}^{\perp q}(x) H_1^{\perp q}(z), \quad (2)$$

$$\sigma_{UT}^{\sin \phi} \propto S_T (1-y) \sin(\phi + \phi_S) \sum_{q,\bar{q}} e_q^2 x h_1(x) H_1^{\perp q}(z), \quad (3)$$

$$+ S_T (1-y + y^2/2) \sin(\phi - \phi_S) \sum_{q,\bar{q}} e_q^2 x f_{1T}^{\perp q}(x) D_1^q(z), \quad (4)$$

where  $\phi$  is the azimuthal angle between the scattering plane formed by the initial and final momenta of the electron and the production plane formed by the transverse momentum of the observed hadron and the virtual photon;  $\phi_S$  is the azimuthal angle of the transverse spin in the scattering plane. The subscripts in  $\sigma_{UL}$  and  $\sigma_{UT}$  specify the beam and target polarizations ( $L$  stands for longitudinally polarized,  $T$  for transversely polarized targets, and  $U$  for unpolarized beam);  $S_L$  and  $S_T$  are longitudinal and transverse components of the target polarization with respect to the direction of the virtual photon.

The SIDIS cross section with a longitudinally polarized target in subleading order contains an additional contribution to the  $\sin \phi$  moment ( $\sigma_{UL}$ ) [10, 33, 34]:

$$\sigma_{UL}^{\sin \phi} \propto S_L \sin \phi (2-y) \sqrt{1-y} \frac{M}{Q} \sum_{q,\bar{q}} e_q^2 x^2 h_L^q(x) H_1^{\perp q}(z), \quad (5)$$

where  $h_L^q(x)$  is the twist-3 distribution function [29].

Measurements of average moments  $\langle W(\phi) \rangle_{UL} = \int \sigma_{UL}(\phi) W(\phi) d\phi / \int \sigma(\phi) d\phi$  ( $W(\phi) = \sin \phi, \sin 2\phi$ ) of the cross section  $\sigma_{UL}^{W(\phi)}$  will single out corresponding terms in the cross section. For spin-dependent moments this is equivalent to the corresponding spin asymmetries  $A_{UL}^W$ . Thus, for example, the  $\sin \phi$  SSA

of the cross section for longitudinally polarized beam and unpolarized target is defined as:

$$\frac{1}{2}A_{LU}^{\sin\phi} = \langle \sin\phi \rangle_{LU} = \frac{1}{P^{\pm}N^{\pm}} \sum_{i=1}^{N^{\pm}} \sin\phi_i,$$

where  $P^{\pm}$  and  $N^{\pm}$  are the polarization and number of events for  $\pm$  helicity state, respectively. The final asymmetry is defined by the weighted average over two independent measurements for both helicity states.

Equations (2) and (3) describe single-spin asymmetries involving the first moment of the Collins fragmentation function integrated over the transverse momentum of the final hadron  $H_1^{\perp q}$ . A unique feature of the Collins mechanism is the presence of a leading twist  $\sin 2\phi$  SSA for a longitudinally polarized target [33]. Measurements of the  $\sin 2\phi$  SSA (see Fig. 3) thus allow one to study the Collins effect with no contamination from other mechanisms. Recent measurement of  $\sigma_{UL}$  by HERMES [20] is consistent with a  $\sin 2\phi$  moment of zero. A sufficiently large effect has been predicted only at large  $x$  [31, 32], a region well-covered by JLab. The leading-twist distribution function  $h_{1L}^{\perp}(x)$ , accessible in this measurement, describes the transverse polarization of quarks in a longitudinally polarized proton.

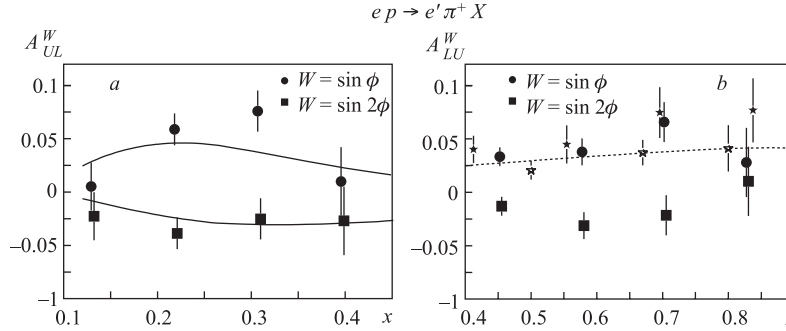


Fig. 3. *a*) Azimuthal moments from CLAS 5.7 GeV polarized target data in a range  $0.5 < z < 0.8$ . Curves are prediction from Ref. 32 for  $\sin\phi$  and  $\sin 2\phi$  SSA in the CLAS kinematics. *b*) Comparison of the  $z$  dependence of  $A_{UL}$  measured at 5.7 GeV with published HERMES data [20] (open stars), and CLAS data at 4.3 GeV (solid stars)

The  $\sin\phi$  moments of the cross section measured with CLAS at 5.7 GeV is in good agreement with the CLAS measurements at 4.3 GeV and the HERMES measurement at 27.5 GeV, which indicates that the asymmetry observables are not sensitive to the beam energy (see Fig. 3). Curve for the  $z$  dependence of  $\sin\phi$  moment is a calculation for HERMES [34] kinematics. Good agreement

of theory and data, both from CLAS and HERMES has been achieved [38] also when analyzing the longitudinal target SSA (Fig. 3, *b*) in terms of the Siverts effect based on the BHS approach with final state interactions [17].

The  $\sin \phi$  moments of the SIDIS cross section with a longitudinally polarized target contain contributions both from the Siverts effect ( $T$ -odd distribution) [6] and the Collins effect ( $T$ -odd fragmentation) [7] and additional measurements are required to separate them. They include SSA measurements with transversely polarized target and measurements with polarized beam and unpolarized target.

The distribution and fragmentation functions responsible for a nonzero beam spin asymmetry in SIDIS were first identified by Levelt and Mulders [28] and Yuan [24]. The contribution from Collins effect includes the interaction-dependent part  $\tilde{e}(x)$  of the twist-3 unpolarized distribution function  $e(x)$  introduced by Jaffe and Ji [29], and the Collins fragmentation function  $H_1^\perp(z)$  [7]. The contribution from Siverts effect includes the leading-twist  $T$ -odd distribution function  $h_1^\perp$  [10] and the twist-3 fragmentation function  $E(z)$ . The  $x$  dependence of beam SSA, thus, is defined either by the ratio of the twist-3 unpolarized distribution function  $e(x)$  or twist-2 distribution function  $h_1^\perp$ , and the leading twist distribution function  $f_1(x)$  [24, 28]:

$$\sigma_{LU}^{\sin \phi} \propto \lambda_e 2y \sqrt{1-y} \sin(\phi) \sum_{q, \bar{q}} e_q^2 x^2 \tilde{e}(x) H_1^{\perp q}(z), \quad (6)$$

$$\sigma_{LU}^{\sin \phi} \propto \lambda_e 2y \sqrt{1-y} \sin(\phi) \sum_{q, \bar{q}} e_q^2 x h_1^{\perp q}(x) E^q(z). \quad (7)$$

One major concern for SIDIS studies at large  $z$  in particular for low beam energies is the small missing mass of the remnant system. The beam spin asymmetry was extracted for two different beam energies as a function of the missing mass of the  $\gamma * p \rightarrow \pi^+ X$  to address that concern. Above the nucleon mass no significant  $M_X$  dependence was observed, indicating that asymmetry is not related to any specific remnant configuration (see Fig. 4).

The measured beam SSA  $A_{LU}^{\sin \phi}$  is positive for a positive electron helicity in the range of  $0.15 < x < 0.4$  (see Fig. 4). It is consistent with CLAS measurements at 4.3 GeV [23], increases with  $z$ , and shows no significant dependence on the  $x$  range (Fig. 4, *b*). This behavior is another indication that factorization is holding.

Beam SSA extracted at 4.3 GeV after correction for a different kinematic prefactor (see Eqs. (6), (7)), which is different at CLAS and HERMES (Fig. 5, *a*) are also consistent with preliminary HERMES data [37] (Fig. 5, *b*) indicating that there is no significant dependence of beam SSA on beam energy.

The  $x$  and  $z$  dependences of the CLAS beam SSA (see Fig. 6) were analyzed by Efremov et al. [32] and Yuan [24] in terms of Collins and Siverts effect (assuming the final state interaction may be responsible for the effects) respectively. A beam spin asymmetry of this magnitude can be also obtained [30] using a

mechanism similar to that proposed by Brodsky, Hwang and Schmidt for the target spin asymmetry case [17] (dotted curve on Fig. 6).

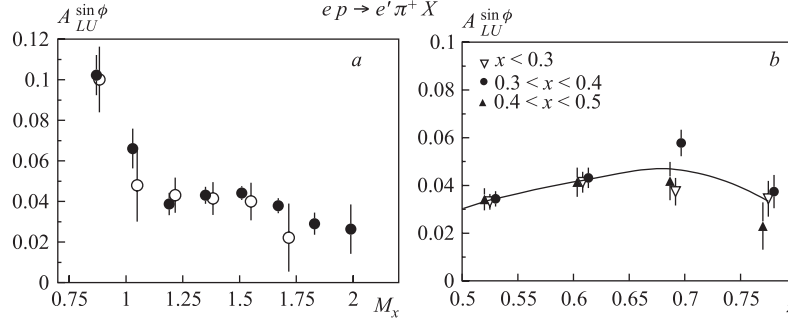


Fig. 4. *a*)  $M_X^2$  dependence of  $A_{LU}$  for beam energies 5.7 GeV (solid circles) and 4.3 GeV (open circles). *b*) The beam-spin azimuthal asymmetry as a function of  $x$  for different  $z$  bins

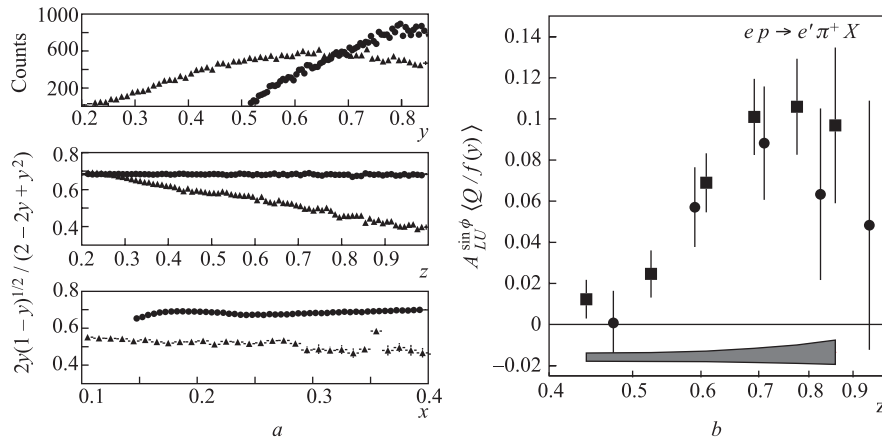


Fig. 5. Kinematic distributions at CLAS (circles) and HERMES (triangles) (*a*) and  $A_{LU}$  (*b*) corrected for the kinematic factor at CLAS (squares) and HERMES (circles)

The first extraction of the twist-3 distribution function from the CLAS beam SSA data has been reported recently by Efremov et al. [31] using a particular parametrization of the Collins fragmentation function. With a certain approximation for the twist-3 functions  $e(x)$  and  $E(z)$ , the beam SSA could become a



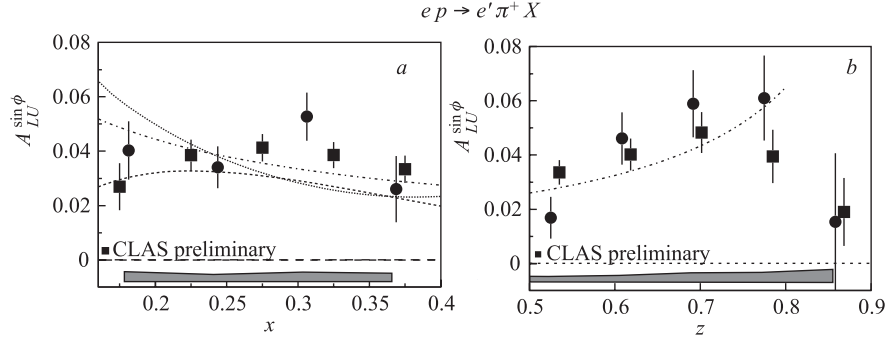


Fig. 6. The beam-spin azimuthal asymmetry ( $\sin \phi$  moment of the cross section) extracted from hydrogen data at 5.7 GeV (squares) and 4.3 GeV (circles) as a function of  $x$  in a range  $0.5 < z < 0.8$  (a) and as a function of  $z$  in a range  $0.1 < x < 0.4$  (b). Curves represent calculations performed assuming only the Sivers effect (dash-dotted lines) [24] or only the Collins effect (dashed line) [32] contributes to  $A_{LU}$

major source of information on the  $T$ -odd distribution ( $h_1^\perp$ ) and fragmentation ( $H_1^\perp$ ) functions.

### 3. SSA IN HARD EXCLUSIVE PRODUCTION OF PIONS

The Deeply Virtual Compton Scattering (DVCS), a process involving a single hadron was identified [3,4] as the cleanest tool in constraining GPDs from data. First experimental results are now available from HERA [39,40], HERMES [41], and CLAS [42] Collaborations. Another important class of processes where GPDs occur is the hard exclusive production of light mesons allowing to filter different GPDs by different final-state hadrons [43]. The beam  $\sin \phi$  SSA for exclusive events in the hard scattering kinematics (see Fig. 7) unlike the case of the target  $\sin \phi$  SSA [44] is positive and compatible with the  $A_{LU}^{\sin \phi}$  for the semi-inclusive sample at large  $z$ . Even though the power corrections for the absolute crosssection of exclusive pion electroproduction analyzed in terms of generalized parton distributions are expected to be large, there are indications of a *precocious scaling* in ratios of observables [45]. At large values of Bjorken  $x$  and  $z$  at fixed  $Q^2$  the contribution of multiparton correlations or higher twist effects increases, eventually leading to a breakdown of the partonic description. Model calculations indicate that SSAs are less sensitive to a wide range of corrections than cross section measurements in both semi-inclusive [46] and in hard exclusive [47,48] pion production. The measurement of spin asymmetries could therefore become a major tool for studying quark transverse momentum-dependent distributions [6–9, 15, 28] and GPDs [47,48] in the  $Q^2$  domain of a few  $\text{GeV}^2$ .

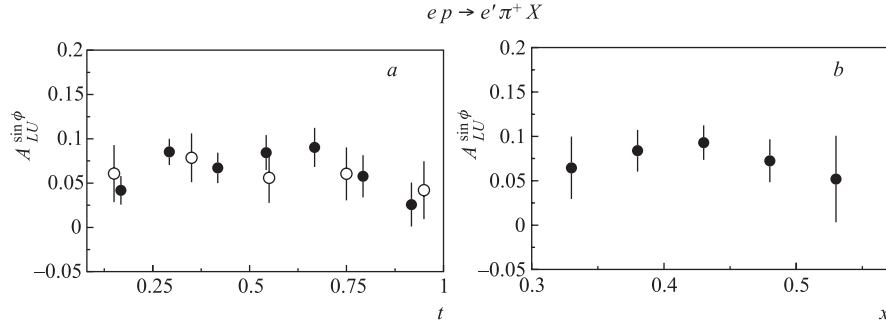


Fig. 7. The beam SSA for exclusive  $\pi^+$  (solid circles) and  $\pi^0$  (open circles) in hard scattering kinematics ( $W^2 > 4$ ,  $Q^2 > 1.5$  with  $\langle Q^2 \rangle \approx 2.5$ ,  $\langle x \rangle \approx 0.34$ ) as a function of  $t$  (a), and as a function of  $x$  for exclusive  $\pi^+$  for  $W^2 > 5$ ,  $Q^2 > 2.5$  with  $\langle Q^2 \rangle \approx 3$  (b)

In conclusion, significant single-spin asymmetries have been observed in semi-inclusive and exclusive electroproduction of pions at JLab. The data from CLAS experiments with 5.7 GeV polarized electrons provide a unique possibility to examine the factorization hypothesis and study kinematic dependences of SSAs in semi-inclusive and exclusive processes in hard-scattering kinematics.

The current CLAS data suggests that the high-energy description of the SIDIS process can be extended to the moderate energies of the CLAS measurements. Measured kinematic dependences of single- and double-spin asymmetries are consistent with a partonic picture, and can be described by a variety of theoretical models. They provide important input for global analysis of observed SSAs, eventually leading to the separation of different contributions and extraction of underlying, essentially unexplored, distribution functions.

#### REFERENCES

1. Ashman J. *et al.* // Phys. Lett. B. 1988. V. 206. P. 364.
2. Muller D. *et al.* // Fortschr. Phys. 1994. V. 42. P. 101.
3. Ji X. // Phys. Rev. Lett. 1997. V. 78. P. 610.
4. Radyushkin A. V. // Phys. Lett. B. 1996. V. 380. P. 417.
5. Ralston J., Soper D. // Nucl. Phys. B. 1979. V. 152. P. 109.
6. Sivers D. // Phys. Rev. D. 1991. V. 43. P. 261.
7. Collins J. // Nucl. Phys. B. 1993. V. 396. P. 161.
8. Mulders P. J., Tangerman R. D. // Nucl. Phys. B. 1996. V. 461. P. 197.
9. Kotzinian A. // Nucl. Phys. B. 1995. V. 441. P. 234.
10. Boer D., Mulders P. // Phys. Rev. D. 1998. V. 57. P. 5780; Nucl. Phys. B. 2000. V. 569. P. 505.

11. Anselmino M., Murgia F. // Phys. Lett. B. 1998. V. 442. P. 470.
12. Collins J. // Phys. Lett. B. 2002. V. 536. P. 43.
13. Brodsky S. et al. // Nucl. Phys. B. 2002. V. 642. P. 344.
14. Ji X., Yuan F. // Phys. Lett. B. 2002. V. 543. P. 66.
15. Belitsky A., Ji X., Yuan F. // Nucl. Phys. B. 2003. V. 656. P. 165.
16. Belitsky A., Ji X., Yuan F. hep-ph/0307383. 2003.
17. Brodsky S. et al. // Phys. Lett. B. 2002. V. 530. P. 99.
18. Heller K. et al. // Proc. of «Spin 96», Amsterdam, Sep. 1996. P. 23.
19. Bravar A. et al. (Fermilab E704 Collab.) // Phys. Rev. Lett. 1996. V. 77. P. 2626.
20. Airapetyan A. et al. (HERMES Collab.) // Phys. Rev. Lett. 2000. V. 84. P. 4047.
21. Airapetyan A. et al. (HERMES Collab.) // Phys. Rev. D. 2001. V. 64. P. 097101.
22. Bravar A. // Nucl. Phys. Proc. Suppl. B. 1999. V. 79. P. 521.
23. Avakian H. et al. (CLAS Collab.). hep-ex/0301005.
24. Yuan F. hep-ph/0310279. 2003.
25. Ji X. // Phys. Rev. D. 1994. V. 49. P. 114.
26. Kretzer S. et al. // Eur. Phys. J. C. 2001. V. 22. P. 269.
27. Mecking B. et al. // Nucl. Instr. Meth. A. 2003. V. 503. P. 513.
28. Levt J., Mulders P.J. // Phys. Lett. B. 1994. V. 338. P. 357.
29. Jaffe R. L., Ji X. // Nucl. Phys. B. 1992. V. 375. P. 527.
30. Afanasev A., Carlson C. hep-ph/0308163.
31. Efremov A. et al. // Nucl. Phys. A. 2002. V. 711. P. 84.
32. Efremov A. et al. // Phys. Rev. D. 2003. V. 67. P. 114014.
33. Kotzinian A. M., Mulders P. J. // Phys. Rev. D. 1996. V. 54. P. 1229.
34. Kotzinian A. M. et al. // Nucl. Phys. A. 2000. V. 666. P. 290–295.
35. Airapetyan A. et al. (HERMES Collab.) // Phys. Lett. B. 1999. V. 464. P. 123.
36. Gluck M. et al. // Phys. Rev. D. 1996. V. 53. P. 4775.
37. Miller A. // Proc. of «Spin 2002», BNL, Upton, USA, 2002.
38. Avakian H., Elouadrhiri L. // Proc. of CIPANP 2003. N. Y., 2003.
39. Saull P. R. B. (ZEUS Collab.). hep-ex/0003030.
40. Adloff C. et al. (H1 Collab.) // Phys. Lett. B. 2001. V. 517. P. 47.
41. Airapetyan A. et al. (HERMES Collab.) // Phys. Rev. Lett. 2001. V. 87. P. 182001.
42. Stepanyan S. et al. (CLAS Collab.) // Ibid. P. 182002.
43. Goeke K. et al. // Prog. Part. Nucl. Phys. 2001. V. 47. P. 401.
44. Airapetyan A. et al. (HERMES Collab.) // Phys. Lett. B. 2003. V. 562. P. 182.
45. Belitsky A. hep-ph/0307256.
46. Bacchetta A. et al. // Phys. Rev. D. 1999. V. 65. P. 094021.
47. Frankfurt L. L. et al. // Ibid. V. 60. P. 014010.
48. Belitsky A., Muller D. // Phys. Lett. B. 2001. V. 513. P. 349.